Energy-efficient small-scale ammonia synthesis process with plasma-enabled nitrogen oxidation and catalytic reduction of adsorbed NOx

Energy-efficient Small-scale Ammonia Synthesis Process with Plasma-enabled Nitrogen Oxidation and Catalytic Reduction of Adsorbed NO_x

Lander Hollevoet,[a] Elise Vervloessem,[b,c] Dr. Yury Gorbanev,[b] Dr. Anton Nikiforov,[c] Prof. Nathalie De Geyter,[c] Prof. Annemie Bogaerts,*[b] Prof. Johan A. Martens*[a]

[a] Lander Hollevoet, prof. Johan A. Martens
Center for Surface Chemistry and Catalysis: Characterization and Application Team
KU Leuven
Leuven BE-3001, Belgium
E-mail: johan.martens@kuleuven.be

[b] Elise Vervloessem, dr. Yury Gorbanev, prof. Annemie Bogaerts
Research Group PLASMANT, Department of Chemistry
University of Antwerp
Wilrijk BE-2610, Belgium
E-mail: Annemie.bogaerts@uantwerpen.be

[c] Elise Vervloessem, dr. Anton Nikiforov, prof. Nathalie De Geyter
Research Unit Plasma Technology (RUPT), Department of Applied Physics, Faculty of Engineering and Architecture
Ghent University, Ghent BE-9000, Belgium

Abstract: Industrial ammonia production without CO_2 emission and low energy consumption is one of the technological grand challenges of this age. Current Haber-Bosch ammonia mass production processes work with a thermally activated iron catalyst needing high pressure. The need of large volumes of hydrogen gas and the continuous operation mode render electrification of Haber-Bosch plants difficult to achieve. Electrochemical solutions at low pressure and temperature are faced with the problematic inertness of the nitrogen molecule on electrodes. Direct reduction of N_2 to ammonia is only possible with very reactive chemicals such as lithium metal, the regeneration of which is energy intensive. Here we show the attractiveness of an oxidative route for N_2 activation. N_2 conversion to NO_x in a plasma reactor followed by reducing it with H_2 on a heterogeneous catalyst at low pressure is an energy-efficient option for small-scale distributed ammonia production with renewable electricity and without intrinsic CO_2 footprint.

Introduction

Industrial ammonia production processes emit large amounts of CO_2. In efficient Haber-Bosch plants using hydrogen gas from steam methane reforming (SMR), the CO_2 emission amounts to ca. 1.7 metric ton per metric ton of ammonia produced.[1] Especially the fertilizer chemical segment of the global ammonia market is forecasted to continue growing with the increasing world population. Electrification of the hydrogen production, avoiding the use of fossil carbon sources, is an obvious way to avoid CO_2 emission and to produce green ammonia. For a Haber-Bosch plant operated at 200-250 bar and 400-500°C, economies of scale are obtained only above 100,000 metric ton per year.[2] Hydrogen production by water electrolysis instead of SMR is an option for such large Haber-Bosch plants but the powering of large electrolysis plants with renewable electricity for massive non-stop ammonia production units is challenging. Smaller scale distributed ammonia production at the pace of variable renewable electricity supply offers a solution,[3] but to achieve this, other concepts besides heterogeneous catalysis at high pressure and temperature are needed to downsize the reactor. Electrolysis of N_2 and H_2 or H_2O is an option, but the development of electrodes activating the inert N_2 molecule under mild reaction conditions does not yet meet with success.[4] Reductive activation of the N_2 molecule is feasible with strong reductants like metallic lithium,[5] chemical looping with alkaline and alkaline earth metals[6] and using plasma processes,[7–10] but the energy need exceeds substantially that of Haber-Bosch processes. Oxidative activation of N_2 molecules to form NO_x and/or nitrate molecules obtained from NO_x is kinetically much easier than reduction. Electrochemical[11] and catalytic technology for the selective reduction of NO_x and nitrate to ammonia is already available.[12,13] Such detour via oxidation to ultimately achieve reduction may seem contradictory, but here we show energy needs are lower and closer to the Haber-Bosch process.

Plasma Nitrogen Oxidation coupled with Catalytic Reduction to Ammonia (PNOCRA) is such an oxidative approach.[13] The process scheme is shown in Figure 1. N_2 from air is oxidized to NO_x using a plasma reactor, and further adsorbed on a Lean NO_x Trap (LNT). Contrary to the automotive application of LNT technology where NO_x needs to be selectively reduced to N_2 for depolluting exhaust gas, here the reduction is aimed at producing NH_3. To achieve the selective reduction of adsorbed NO_x to ammonia, the H_2 gas needed can be produced by water electrolysis. An LNT is operated in a cyclic mode with NO_x trapping alternating with chemical reduction. To achieve continuous ammonia production, at least two LNT units alternating between NO_x trapping and chemical reduction mode are needed, as shown in Figure 1. The number of required LNT's depends on the ratio of adsorption and reduction time.

Based on literature data on the energy need of NO_x production in plasma reactors using the old Birkeland-Eyde process,[14] state-of-the-art LNT performances[15] and the use of green hydrogen,

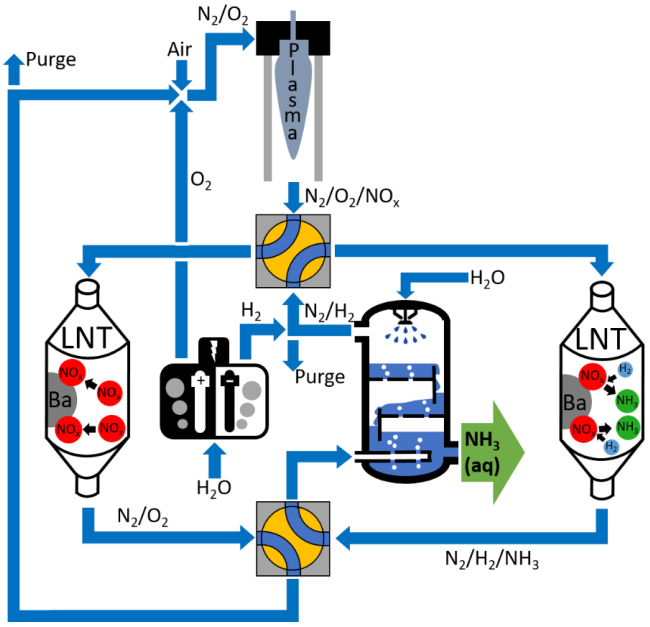

Figure 1. PNOCRA process scheme, where NO_x is produced from air in a plasma reactor and selectively adsorbed on a Lean NO_x Trap (LNT). After saturation, the adsorbed NO_x is catalytically reduced to ammonia, regenerating this way the LNT. Two LNT units alternating between adsorption and reduction modes are needed for continuous ammonia synthesis.

the energy cost for ammonia production with PNOCRA previously was estimated at 4.6 MJ mol^{-1}.[13] In this work we present experimental data on a dedicated optimized plasma-LNT combination with a drastic decrease of the energy cost to only 2.1 MJ mol^{-1}, making it, to the best of our knowledge, the lowest energy cost for decentralized small-scale green ammonia production reported so far.

Results and Discussion

Plasma process for the conversion of air to NO_x

Plasma experiments were performed with a pulsed plasma jet operating in air, i.e. the so-called Soft Jet, originally developed for biomedical applications.[16,17] Obtained NO, NO_2 and total NO_x concentrations with the plasma reactor at different gas flow rates are presented in Figure 2. The NO_x concentration in the outlet decreases from ca. 1200 ppm to ca. 150 ppm when increasing the gas flow rate from 0.2 to 2 L min^{-1}, shortening this way the residence time in the plasma (Figure 2a). The NO_x is composed mainly of NO. NO_2 being a secondary product derived from NO remains more or less constant at a low concentration. By-products such as O_3, N_2O_5, N_2O_3, N_2O and NO_3 were not detected at any of the conditions investigated (FTIR spectra can be found in the supporting information, Figure S3).

Based on equilibrium composition calculations in air as a function of temperature, we can deduce that the NO produced by our plasma jet at the lowest flow rate approaches the thermal NO yield of 1000 – 1200 ppm at 1750 K,[18,19] while the NO_2 produced exceeds the equilibrium NO_2 concentration, which was reported to be negligible at this temperature. However, one must keep in mind that the plasma jet only operates at 1750 K for a very short period of time, resulting in an average temperature between 300 – 330 K.[9] This means that our plasma jet exceeds the equilibrium concentrations, because it uses a pulsed plasma, which enables non-equilibrium conditions and keeps the average temperature low.

The NO_x production rate is around 20 – 30 mg h^{-1} (Figure 2b). Based on this NO_x production rate and plasma power (P; see below), the energy cost (EC) of NO_x formation can be calculated as follows:

$$EC\ \left[\frac{MJ}{mol}\right] = \frac{P[W]}{mol\ of\ NO_x\ produced\ per\ second\ [mol/s]} \cdot \frac{1}{10^6[J/MJ]} \qquad (1)$$

The energy cost decreases from ca. 0.61 MJ mol^{-1} to ca. 0.43 MJ mol^{-1} with increasing flow rate in the range 0.2 L min^{-1} to 2 L min^{-1} (Figure 2). The lowest value of 0.42±0.03 MJ mol^{-1} is reached at 1.5 L min^{-1}. To the best of our knowledge, a value of 0.42 MJ mol^{-1} is the lowest EC reported in literature for atmospheric-pressure plasma-based NO_x production. A literature review of NO_x production rates and EC values in various plasma types was recently published by Rouwenhorst et al.[20] Plasma reactors operating at atmospheric pressure typically produce NO_x at concentrations in the percentage range with an EC in a very wide range, from 2.4 to 1,700 MJ mol^{-1} (see[20]). The lowest EC at atmospheric pressure of 2.4 MJ mol^{-1} reported up to now was obtained long time ago in the industrial Birkeland-Eyde process, which produced 1-2 % NO in a thermal arc plasma.[14] In recent years various atmospheric-pressure plasmas have been

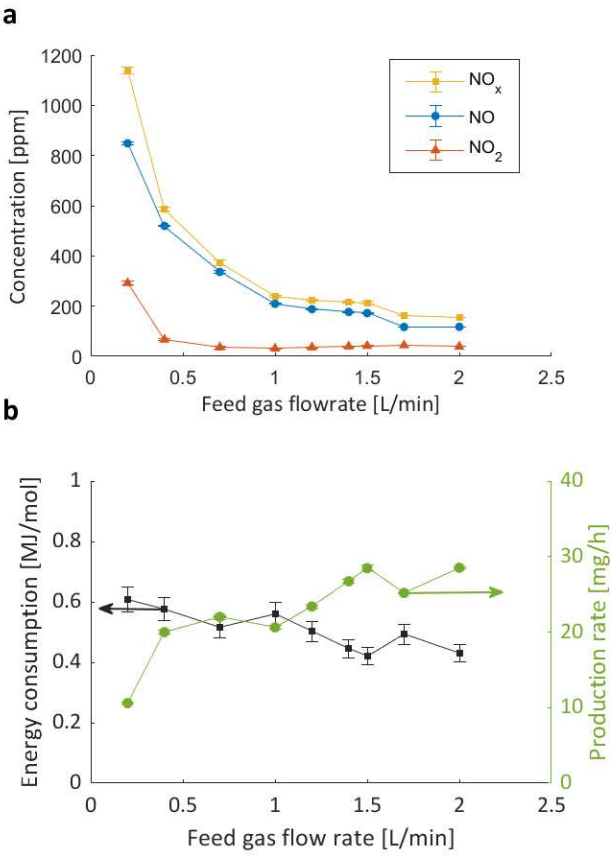

Figure 2. Performance of the plasma reactor, with (a) NO, NO_2 and total NO_x concentration as measured by FTIR in the reactor outlet depending on gas flow rate and (b) Corresponding energy consumption and NO_x production rate. Error bars represent standard deviations

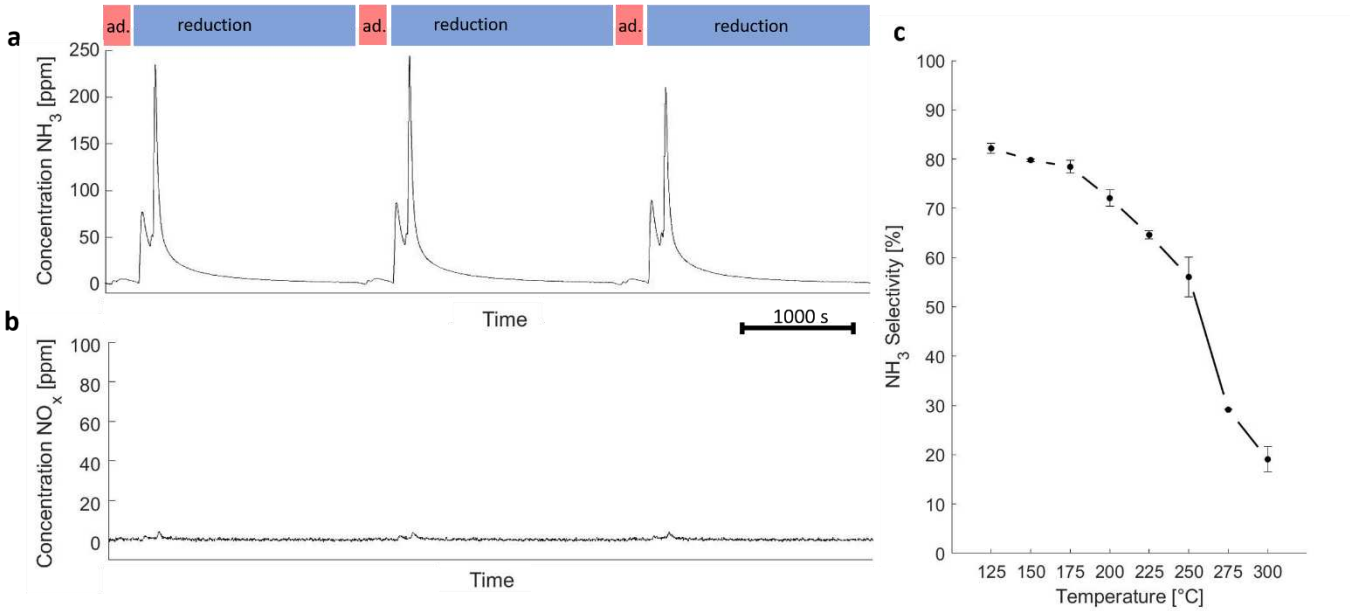

Figure 3. Performance of the Pt/BaO/Al_2O_3 LNT. (a & b) show the outlet concentration of (a) NH_3 and (b) NO_x during three consecutive adsorption-reduction cycles at 175°C. Adsorption phase was executed with a gas mixture composed of 200 ppm NO, 20 % O_2 and 80 % N_2, reduction phase with a gas mixture composed of 5 % H_2 and 95 % N_2. (c) Shows the NH_3 selectivity of the NO_x reduction at different temperatures. Error bars represent standard deviations.

investigated, such as spark discharges,[21] radio-frequency discharges,[22] corona discharge,[23] glow discharges,[24] (packed bed) dielectric barrier discharges,[25] different types of arc discharges, including pulsed arc and various gliding arc plasmas.[26–29] The lowest EC's were typically obtained in gliding arc plasma reactors (2.4 – 3.6 MJ mol^{-1}).[26–29] Hence, our reported EC of 0.42 MJ mol^{-1} is drastically better than the state-of-the-art of atmospheric pressure plasma reactors. The superior performance is ascribed to the pulsed regime, causing clear vibrational non-equilibrium.[30,31] Microwave plasmas at reduced pressure (0.01 – 0.07 bar) produce NO_x at low EC,[32–34] similar to our present work with the pulsed Soft Jet plasma at atmospheric pressure, but for fair comparison the energy requirements to reduce the pressure and for cooling at low pressure should be added.

As a side note, using a plasma-catalytic process can be envisaged. The reports available to date describe a combination of plasma with heterogeneous catalysts (both downstream and inside the active plasma compartment) which achieve a plasma-catalysis synergy, reducing the energy consumption of nitrogen fixation.[25,35,36] While the exact nature of such synergy remains an open question and likely depends on each specific case (e.g., plasma parameters), we can hypothesize the possibility of coupling our plasma process with catalysis to further decrease the EC of our plasma-based nitrogen oxidation process.

Based on the tradeoff between energy need and product concentrations in the plasma reactor (Figure 2), the product gas with a NO_x concentration of ca. 200 ppm, obtained at the lowest energy cost of 0.42 MJ mol^{-1} was considered for being converted on a downstream Lean NO_x Trap (LNT) of the PNOCRA process.

NO_x separation and reduction to NH_3 on Lean NO_x Trap

Lean NO_x Traps have been developed in the automotive industry for exhaust gas after-treatment of lean burn engines. Their purpose is to filter out the NO_x molecules and to reduce them catalytically to N_2 using a spike of CO, hydrocarbons and H_2 reductants, produced by the engine running for a short time in fuel-rich mode. H_2 is known to be the most reactive at the lowest temperatures, and typically yields the highest selectivity towards NH_3 under such conditions.[37] The LNT contains barium oxide and finely dispersed platinum metal to provide NO_x adsorption and redox catalytic activity, respectively. NO_2 is the adsorbed NO_x species. NO needs catalytic oxidation with O_2 over platinum in order to be adsorbed. NO_2 adsorption proceeds via disproportionation of NO_2 to form barium nitrate and NO (Equation (2)). Under reducing conditions, barium nitrate becomes thermodynamically unstable and decomposes, producing NO_x which is reduced to N_2 over the platinum catalyst (Equation (3)). The LNT concept needs adaptation to suit the PNOCRA process since the NO_x reduction catalyst needs to favor the formation of NH_3 over N_2 (Equation (4)).

$$3\ NO_2 + BaO \rightarrow Ba(NO_3)_2 + NO \quad (2)$$

$$Ba(NO_3)_2 + 5\ H_2 \rightarrow BaO + N_2 + 5\ H_2O \quad (3)$$

$$Ba(NO_3)_2 + 8\ H_2 \rightarrow BaO + 2\ NH_3 + 5\ H_2O \quad (4)$$

LNT material was prepared by loading alumina support with barium oxide and platinum at a weight ratio for Pt/BaO/Al_2O_3 of 1/20/100. A fixed bed of LNT pellets was loaded in a packed bed reactor and subjected to adsorption-reduction N_2. Reduction was done using a gas mixture with cycles. The NO_x bearing product gas of the plasma reactor at optimum operation was simulated with a gas mixture containing 200 ppm NO, 20 % O_2 and 80 % N_2. Reduction was done using a gas mixture with 5 % H_2 in N_2. Adsorption-reduction cycles were performed isothermally at temperatures in the range of 125-300°C. Several cycles were performed at each temperature. At temperatures below 125°C, both the adsorption of NO_x and the desorption of ammonia from the catalyst surface become kinetically challenging.

The performance of the LNT in consecutive cycles was very reproducible, which is illustrated for the temperature of 175°C in

Figure 3a and b. NO_x fed to the LNT during 250 seconds was quantitatively adsorbed since virtually no NO_x was detected in the outlet (Figure 3b). After switching to the reduction mode, ammonia was formed desorbing readily (Figure 3a). The peak has a split, which likely is due to a complex interplay of formation and adsorption fronts in the fixed bed of LNT adsorbent-catalyst combination. The selectivity for NO_x to ammonia conversion at 175°C amounted to 78 % (Figure 3c) with a high average NH_3 production rate of 0.077 mmol h^{-1} g_{LNT}^{-1}, or 10.2 mmol h^{-1} g_{Pt}^{-1} over the course of an absorption/reduction cycle. N_2 was the only by-product. The formation of N_2O was below the detection limit (< 1 ppm). Temperature matters to performance. At the lowest temperatures of 125 and 150°C, some NO breakthrough occurred probably because of incomplete catalytic oxidation of NO to NO_2 at these low temperatures.

At 175°C and higher temperatures, all fed NO_x was quantitatively adsorbed and converted (Figure 3b). The selectivity to ammonia was highest at 125°C (82%) and decreases with reaction temperature (Figure 3c). In the reduction reaction of NO_x to N_2, NH_3 is a reaction intermediate.[38–40] This decrease of ammonia selectivity with increasing reaction temperature is explained by the larger extent of consecutive reaction caused by enhanced catalytic activity.

The LNT catalyst shows excellent stability during a series of 11 consecutive adsorption/desorption cycles (Figure S2). This observation is expected as Lean NO_x Traps used in the car industry survive for many years in much more harsh conditions, with frequent heating up and cooling down, higher temperatures and the presence of other gaseous compounds like traces of SO_2 and CO and large concentrations of H_2O. These factors point towards a very long lifetime for the LNT catalysts.

Furthermore, the Lean NO_x Traps are known to operate at much lower H_2 concentrations, which shows the great activity of the LNT catalyst. Figure S1 shows how the adsorbed NO_x reduces quickly to NH_3 at hydrogen concentrations as low as 1000 ppm.

A comprehensive comparison of the performance of the LNT with other approaches for the reduction of oxidized N to ammonia is provided in Table S2.

NH_3 product separation and applications

After reduction in the Lean NO_x Trap, the ammonia product is separated out of the N_2/H_2 gas phase in a washing column. Ammonia is highly soluble in water, with concentrations up to 30 wt % in standard conditions, while N_2 and H_2 both have a very low solubility of only 0.00016 wt% and 0.002 wt% respectively.

This approach is different from the industrial Haber-Bosch process, which separates anhydrous ammonia in a high pressure condenser and requires energy for refrigeration. Because the Haber-Bosch process is highly centralized, while fertilizer consumption is decentralized, ammonia is typically converted into an easily transportable solid product. Most common end products are urea ($CO(NH_2)_2$) and ammonium nitrate (NH_4NO_3), which are produced by the Bosch-Meiser or Ostwald processes. These downstream processes require an anhydrous ammonia feed.

Decentralized ammonia production processes like PNOCRA operate at atmospheric pressures and produce a much more dilute product. This avoids the presence of hazardous and corrosive anhydrous ammonia, which needs to be stored under pressures of at least 8 bar. It also makes atmospheric pressure processes incompatible with downstream processes for production of solid fertilizers. Atmospheric pressure processes can therefore not replace Haber-Bosch in centralized fertilizer production plants, but lower product concentrations are much less problematic in a decentralized approach. The aqueous ammonia solution produced by the PNOCRA process can be used directly in fertigation, where fertilizers are dissolved in irrigation water, or hydroculture, where plants grow directly in water containing the necessary nutrients. These techniques are already widely applied for the cultivation of many types of fruits and vegetables. Typical N concentrations range from 50 up to 350 ppm, depending on crop type.[3]

Energy cost and installation cost of ammonia production with PNOCRA

The PNOCRA process scheme (Figure 1) comprises a plasma reactor, two LNT's, a water electrolyzer and a washing column. Out of these unit operations, the plasma reactor and water electrolyzer are responsible for the electricity consumption. The heating of LNT's can be obtained from the exothermal NO_x reduction reaction under adiabatic conditions. The energy cost of running the washing column for separating ammonia from the other gaseous products is negligible compared to the plasma and electrolysis processes.

The total energy cost of the PNOCRA process is the sum of the energy consumed by the plasma reactor and the production of hydrogen by the electrolyzer. The absorption of NH_3 in the washing column and the adsorption and reduction of NO_x on the LNT are spontaneous and therefore do not require additional energy. The optimized plasma reactor consumes 0.42 MJ mol NO_x^{-1}. Assuming that the LNT converts NO_x to ammonia with a selectivity of 80 %, the plasma reactor needs to produce 20 % more NO_x than used effectively for ammonia synthesis. This brings the energy consumption of the plasma process to 0.53 MJ mol NH_3^{-1}. According to reaction stoichiometries, 4 and 2.5 mol H_2 is needed to convert 1 mol NO_x to NH_3 and N_2, respectively. At an NH_3 selectivity of 80 %, 4.6 mol H_2 is required to produce 1 mol NH_3. If H_2 is produced by water electrolysis using an electrolyzer with a typical energy efficiency of 70 %, the electrolyzer consumes ca. 1.57 MJ mol NH_3^{-1}. This brings the total energy cost of the PNOCRA process to a total of ca. 2.1 MJ mol NH_3^{-1}, making PNOCRA the least energy consuming small-scale ammonia production process at mild conditions demonstrated so far. The selectivity of the NO_x reduction reaction on the LNT's matters a lot to the energy need to provide the NO_x and the H_2 needed for the reaction. N_2 by-product formation causes a waste of NO_x and H_2. Enhancing the LNT selectivity to 100 % would already lower the energy need to ca. 1.8 MJ mol NH_3^{-1}. This could be done by finetuning the catalyst and the reaction conditions.

Li-mediated N_2 reduction and plasma processes are alternatives for small scale NH_3 synthesis. The Li-mediated approach was demonstrated at ambient conditions by Lazouski et al.[41] with an energy cost of 12.4-25.5 MJ mol NH_3^{-1}. Energy losses were mainly caused by a large electrolyte resistance, leading to high cell voltages of 20-30 V. Suryanto et al.[42] recently reported Li-mediated NH_3 synthesis from N_2 and H_2 under increased pressure (10-20 bar) with an NH_3 selectivity of 69 % and a cell voltage of ca. 5 V. Including the required energy for H_2 synthesis via electrolysis brings the energy cost to 2.9 MJ mol NH_3^{-1}. The direct conversion of N_2 and H_2 to NH_3 in a plasma reactor was reported by Aihara et al.[43] at an energy cost of 19.1 MJ mol^{-1} (including H_2 production). A combination of plasma NO_x and electrocatalytic

reduction to NH_3 was reported by Sun et al.[11] with an energy cost of 15.5 MJ mol^{-1}. Hence, our reported energy cost of 2.1 MJ mol NH_3^{-1} is lower than any other state-of-the-art approach for small-scale NH_3 production under mild conditions.

Besides energy cost, the installation cost of the PNOCRA process is also a determining factor in economic viability. In this early stage of development, a detailed techno-economic analysis of the process cannot be done accurately, but a more qualitative understanding of equipment cost can be interesting. Compared to the Haber-Bosch process, PNOCRA makes use of much lower pressures and avoids corrosive substances like anhydrous ammonia. This enables the use of low cost materials for piping etc.

Compared to other small-scale processes with plasma NO_x and electrochemical reduction of nitrates, the reaction conditions of PNOCRA are very similar. Both processes also require a plasma reaction for NO_x generation and a washing column, either for NO_x absorption or NH_3 absorption. Ammonia can be directly absorbed in water, but the absorption of NO_x in water prior to electrochemical reduction is more challenging on an industrial scale. It requires both NO_2 absorption and NO oxidation to NO_2. For every two molecules of NO_2 absorbed, one reacts back to NO and needs to be reoxidized. Industrial NO_x absorption columns therefore require alternating oxidation and absorption stages, which makes the column larger and more complex.[44] Another big difference is the need for a LNT in the PNOCRA process or a nitrate reduction electrolyzer for the plasma and electrochemical combination process. However, further research is required to determine which technology will be most cost efficient.

Within the view of future scale-up and transfer of the proposed process to industry, working at increased pressure to increase the amount of moles treated should logically be considered. However, at the moment it is not straightforward how to increase the pressure while maintaining non-equilibrium in the plasma. Indeed, the vibrational non-equilibrium plays a crucial role in the low energy consumption.[45] Although in theory increased pressure would improve the energy consumption, this would also thermalize and constrict the plasma, quenching the vibrational non-equilibrium.

Conclusion & Outlook

For the PNOCRA process demonstrated in this work there is still ample margin for further improvement. One goal is to increase the outlet NO_x concentration of the plasma reactor while maintaining a low energy consumption by plasma reactor design improvements. NO_x adsorption and NH_3 synthesis are decoupled by two separate process steps, so NO_x concentration does not influence the concentration of NH_3 product directly. However, a drastic increase in NO_x concentration would greatly enhance ease of operation as much lower gas volumes would have to be sent over the LNT. LNT technology has been optimized for depollution of engine exhaust, handling NO_x at parts per million quantities, while in PNOCRA the aim is to convert a concentrated stream of NO_x produced in the plasma process. Targeted is a concentrated stream of NH_3, preferably in the range of percentages to facilitate product separation and to downscale the reactor volume. Adapting the LNT catalyst and/or reduction protocol can help reach this goal.

Another goal is to increase the production rate of the catalyst. The most straightforward way to achieve this is by enhancing the catalyst to ensure a faster NH_3 desorption, enabling a shorter cycle time.

A green Haber-Bosch process running with hydrogen from water electrolysis has an energy need of ca. 0.7 MJ mol^{-1}.[46] This is still lower than the current state of PNOCRA, and the oxidative detour is an intrinsic difference. Other aspects but energy may cause a game change. Due to high pressure and exothermicity, Haber-Bosch reactors are difficult to miniaturize. Existing Haber-Bosch plants produce 300,000 to 600,000 metric ton $year^{-1}$, some even up to 1,000,000 metric ton $year^{-1}$.[47] Powering such a large energy-intensive process with decentralized renewable energy sources like solar and wind is very challenging. The Haber-Bosch process also requires steady state operation, which causes problems in combination with intermittent renewable energy supply. Contrary to Haber-Bosch the PNOCRA process is operated under mild temperature and pressure conditions. This can greatly reduce reactor investment costs, which could balance for a higher operational cost due to a higher energy consumption. The components of PNOCRA can also cope well with energy supply fluctuations, making it a better fit for intermittent renewable energy sources. Introduction of small-scale decentralized ammonia plants could contribute to global sustainability since fertilizer demand as well as green electricity production are decentralized. The growing ammonia market could be supplied by small-scale decentralized ammonia plants complementing production in the existing large Haber-Bosch plants.

Experimental Section

Plasma NO_x experiments

Details of the plasma jet set-up can be found in [9]. Briefly, the plasma source consists of a powered needle electrode, surrounded by a quartz capillary, which acts as dielectric spacer between the needle electrode and an outer metal tube. The latter is the grounded electrode, and has a nozzle at the top. The feed gas (compressed dry air; Air Liquide Alphagaz 1, purity ≥ 99.999%) is introduced through the quartz capillary and leaves the jet via the nozzle tip. The gas flow rate was varied from 0.2 to 2 L min^{-1}, and was controlled by a Bronkhorst EL-FLOW® *F-201CV* mass flow controller. This plasma jet produces short (26.3 ms) "trains" of pulses, each time followed by a long pulse-off time (149.9 ms). Detailed diagnostics of the Soft Jet are found elsewhere.[9] Within this pulse train, the spark discharge plasma exists only during short pulses (0.74 µs), as revealed by short voltage and current peaks on top of a sinusoidal waveform. In between these short pulses, no light is emitted, as confirmed by optical emission spectrometry.[9] Therefore the power absorbed into the plasma is calculated using Equation (5), where V and I are the voltage and current values, respectively. Δt is the pulse duration and η is the duty cycle of one pulse train (14.9%).

$$P_{plasma} = \frac{1}{\Delta t} \cdot \int_{pulse\ start}^{pulse\ end} VI\ dt \cdot \eta \qquad (5)$$

The resulting absorbed plasma power (expressed in energy consumed per second, or W) is only 0.1 W. The detailed power calculation is described in recent publications.[9,45] We emphasize that the EC reported in this work is calculated based specifically on the power absorbed in plasma, which is the standard approach in plasma research.[45,48] This means the displacement current during the pulse is not considered.

We acknowledge that the loss of the rest of the power of the pulse within the pulse train (which corresponds to the resistive, capacitive, and inductive losses) can be reduced through optimization of the power supply's coupling to plasma. For example, a recent publication[48] shows a more optimized pulsed plasma power supply. However, such study was beyond the scope of the resent work. It is also important to note that this plasma power is different from the applied power. The applied power going

into the system is 0.76 W. In plasma research, the plasma power (in this case 0.1 W) is always used to calculate the energy cost, as the focus is on the plasma process efficiency. In other words, the efficiency of the power supply is not accounted for, as the latter is the research field of electrical engineering. Reporting the use of the plasma-absorbed power (0.1 W) is therefore necessary, as using the applied power going into the system would render comparison with other works impossible. For practical implementation in industry, however, the power supply efficiency should also be considered. Detailed diagnostics of the Soft Jet can be found in an earlier paper.[9]

Quantitative analysis of the NO, NO_2, N_2O_5, N_2O, and O_3 concentrations in the gas stream was performed on-line with Fourier-transform infrared spectroscopy (FTIR a Matrix-MG2 Bruker FTIR spectrometer). The optical path length inside the gas cell was 5 m and the absolute calibrations were performed by the supplier. We took 50 scans with a resolution of 0.5 cm^{-1} to obtain the FTIR spectra. All plasma experiments were performed in triplicate. The gas composition was averaged over a 15 min measurement period. The concentrations and error bars are the weighted average of the set of three measurements. In between two measurements, the Soft Jet was flushed with air for at least 15 min.

Lean NO_x Trap experiments

Pellets of γ-Al_2O_3 (Alfa Aesar) were crushed and sieved. The particle fraction of 125-250 µm was calcined in air at 500°C for 5 h. Platinum was loaded using aqueous solution of H_2PtCl_6 • 6 H_2O (Merck, 99.95 %) according to the incipient wetness impregnation method, followed by a calcination step in air at 500°C for 5 h. After cooling Barium acetate (Merck, 99 %) was loaded also by incipient wetness impregnation, followed by another calcination step in air at 500°C for 5 h. Finally, the particles were sieved again and the 125-250 µm fraction is kept for use as LNT to ensure plug flow through the particle bed. The nominal weight ratios of Pt to BaO and Al_2O_3 were 1/20/100.

An amount of 60 mg of Pt/BaO/Al_2O_3 catalyst particles was loaded into a quartz tube with an inner diameter of 4 mm and placed into the reactor set-up in vertical position. The powder bed was supported by a plug of quartz wool. Details on the automated reactor can be found in ref [49]. The gasses were supplied by Air Liquide (N_2 purity ≥ 99.999 %; O_2 ≥ 99.5 %; NO (5 % NO in He) ≥ 99.999 %). In a NO_x adsorption/reduction cycle first a mixture of 200 ppm NO and 2 % H_2O in synthetic air (20 % O_2 and 80 % N_2) was conducted over the LNT for 250 s. After flushing with N_2 for 120 s, the reduction of the trapped NO_x was performed using a gas mixture with 5 % H_2 and 0.2 % H_2O in N_2 carrier gas. The gas flowrate was 6 L h^{-1}, corresponding to a GHSV of ca. 60,000 h^{-1}.

The LNT was subjected to three adsorption/reduction cycles at 350°C before starting the reported measurements.

In experiments at the lowest investigated reaction temperatures of 125°C and 150°C, part of the ammonia remained adsorbed. In those experiments, a heating at 10°C min^{-1} up to 250°C was applied to collect all ammonia.

The NO, NO_2 and NH_3 concentration in the gas stream was analyzed on-line using a ABB AO2020-Limas11HW UV photometer, and the N_2O concentration using an ABB AO2020-URAS26 NDIR instrument.

Acknowledgements

We gratefully acknowledge financial support by the Flemish Government through the Moonshot cSBO project P2C (HBC.2019.0108). J.A.M. and A.B. acknowledge the Flemish Government for long-term structural funding (Methusalem). J.A.M. acknowledges KU Leuven for an internal grant by the Industrial Research Fund (No. C3/20/067). A.B. and N.D.G. acknowledge financial support by the Excellence of Science FWO-FNRS project (FWO grant ID GoF9618n, EOS ID 30505023). A.B. also acknowledges financial support by the European Research Council (ERC) under the European Union's Horizon 2020 research and innovation programme (grant agreement No 810182 – SCOPE ERC Synergy project).

Keywords: Plasma Chemistry • Nitrogen oxides • NOx Storage Catalyst • Green Ammonia • Process Electrification

[1] C. Smith, A. K. Hill, L. Torrente-Murciano, *Energy Environ. Sci.* **2020**, *13*, 331–344.

[2] A. Sánchez, M. Martín, *Sustain. Prod. Consum.* **2018**, *16*, 176–192.

[3] B. M. Comer, P. Fuentes, C. O. Dimkpa, Y. Liu, C. A. Fernandez, P. Arora, M. Realff, U. Singh, M. C. Hatzell, A. J. Medford, *Joule* **2019**, *3*, 1578–1605.

[4] J. Choi, B. H. R. Suryanto, D. Wang, H. L. Du, R. Y. Hodgetts, F. M. Ferrero Vallana, D. R. MacFarlane, A. N. Simonov, *Nat. Commun.* **2020**, *11*, 1–10.

[5] S. Z. Andersen, M. J. Statt, V. J. Bukas, S. G. Shapel, J. B. Pedersen, K. Krempl, M. Saccoccio, D. Chakraborty, J. Kibsgaard, P. C. K. Vesborg, et al., *Energy Environ. Sci.* **2020**, *13*, 4291–4300.

[6] W. Gao, J. Guo, P. Wang, Q. Wang, F. Chang, Q. Pei, W. Zhang, L. Liu, P. Chen, *Nat. Energy* **2018**, *3*, 1067–1075.

[7] K. H. R. Rouwenhorst, Y. Engelmann, K. Van 'T Veer, R. S. Postma, A. Bogaerts, L. Lefferts, *Green Chem.* **2020**, *22*, 6258–6287.

[8] A. Anastasopoulou, R. Keijzer, B. Patil, J. Lang, G. Van Rooij, V. Hessel, *J. Ind. Ecol.* **2020**, *24*, 1171–1185.

[9] Y. Gorbanev, E. Vervloessem, A. Nikiforov, A. Bogaerts, *ACS Sustain. Chem. Eng.* **2020**, *8*, 2996–3004.

[10] L. R. Winter, J. G. Chen, *Joule* **2021**, *5*, 300–315.

[11] J. Sun, D. Alam, R. Daiyan, H. Masood, T. Zhang, R. Zhou, P. J. Cullen, E. C. Lovell, A. Jalili, R. Amal, *Energy Environ. Sci.* **2021**, *14*, 865–872.

[12] H. Michel-Kim, H. Pilgrimm, *Process and Device for the Production of Nitrogen Fertiliser and Nitrogen-Enriched Biomass from Air*, **1984**, DE3440190_A1.

[13] a) L. Hollevoet, F. Jardali, Y. Gorbanev, J. Creel, A. Bogaerts, J. A. Martens, *Angew. Chemie - Int. Ed.* **2020**, *59*, 23825–23829.
b) L. Hollevoet, F. Jardali, Y. Gorbanev, J. Creel, A. Bogaerts, J. A. Martens, *Angew. Chem.* **2020**, *132*, 24033-24037.

[14] K. R. Birkeland, *Trans. Faraday Soc.* **1906**, *2*, 98–116.

[15] R. D. Clayton, M. P. Harold, V. Balakotaiah, C. Z. Wan, *Appl. Catal. B Environ.* **2009**, *90*, 662–676.

[16] P. Shaw, N. Kumar, H. S. Kwak, J. H. Park, H. S. Uhm, A. Bogaerts, E. H. Choi, P. Attri, *Sci. Rep.* **2018**, *8*, 1–10.

[17] P. Attri, J. H. Park, J. De Backer, M. Kim, J. H. Yun, Y. Heo, S. Dewilde, M. Shiratani, E. H. Choi, W. Lee, et al., *Int. J. Biol. Macromol.* **2020**, *163*, 2405–2414.

[18] J. Prager, G. Baldea, U. Riedel, J. Warnatz, in *21st ICDERS*, Poitiers, **2007**, pp. 1–4.

[19] S. J. Henderson, J. A. Menart, *J. Thermophys. Heat Transf.* **2008**, *22*, 718–726.

[20] K. H. R. Rouwenhorst, F. Jardali, A. Bogaerts, L. Lefferts, *Energy Environ. Sci.* **2021**, *14*, 2520–2534.

[21] M. Janda, V. Martišovitš, K. Hensel, Z. Machala, *Plasma Chem. Plasma Process.* **2016**, *36*, 767–781.

[22] M. J. Pavlovich, T. Ono, C. Galleher, B. Curtis, D. S. Clark, Z. Machala, D. B. Graves, *J. Phys. D. Appl. Phys.* **2014**, *47*, 505202.

[23] W. Bian, X. Song, J. Shi, X. Yin, *J. Electrostat.* **2012**, *70*, 317–326.

[24] X. Pei, D. Gidon, D. B. Graves, *J. Phys. D. Appl. Phys.* **2020**, *53*, 1–11.

[25] B. S. Patil, N. Cherkasov, J. Lang, A. O. Ibhadon, V. Hessel, Q.

Wang, *Appl. Catal. B Environ.* **2016**, *194*, 123–133.
[26] E. Vervloessem, M. Aghaei, F. Jardali, N. Hafezkhiabani, A. Bogaerts, *ACS Sustain. Chem. Eng.* **2020**, *8*, 9711–9720.
[27] F. Jardali, S. van Alphen, J. Creel, H. A. Eshtehardi, M. Axelsson, R. Ingels, R. Synders, A. Bogaerts, *Green Chem.* **2021**, *23*, 1748–1757.
[28] B. S. Patil, F. J. J. J. Peeters, G. J. van Rooij, J. A. Medrano, F. Gallucci, J. Lang, Q. Wang, V. Hessel, *AIChE J.* **2018**, *64*, 526–537.
[29] W. Wang, B. Patil, S. Heijkers, V. Hessel, A. Bogaerts, *ChemSusChem* **2017**, *10*.
[30] S. Van Alphen, V. Vermeiren, T. Butterworth, D. C. M. Van Den Bekerom, G. J. Van Rooij, A. Bogaerts, *J. Phys. Chem. C* **2020**, *124*, 1765–1779.
[31] S. Van Alphen, F. Jardali, J. Creel, G. Trenchev, R. Snyders, A. Bogaerts, *Sustain. Energy Fuels* **2021**, *5*, 1786–1800.
[32] L. S. Polak, A. A. Ovsiannikov, D. I. Slovetsky, F. B. Vurzel, *Theoretical and Applied Plasma Chemistry*, **1975**.
[33] R. I. Asisov, V. K. Givotov, V. D. Rusanov, A. Fridman, *Sov. Phys., High Energy Chem.* **1980**, *14*, 366.
[34] B. Mutel, O. Dessaux, P. Goudmand, *Rev. Phys. Appliquée* **1984**, *19*, 461–464.
[35] X. Fan, S. Kang, J. Li, T. Zhu, *Water. Air. Soil Pollut.* **2018**, *229*, 1–12.
[36] H. Ma, R. K. Sharma, S. Welzel, M. C. M. van de Sanden, M. N. Tsampas, W. F. Schneider, *Nat. Commun.* **2022**, *13*, 402.
[37] P. Dasari, R. Muncrief, M. P. Harold, *Top. Catal.* **2013**, *56*, 1922–1936.
[38] L. Lietti, I. Nova, P. Forzatti, *J. Catal.* **2008**, *257*, 270–282.
[39] I. Nova, L. Lietti, P. Forzatti, *Catal. Today* **2008**, *136*, 128–135.
[40] C. D. DiGiulio, J. A. Pihl, J. S. Choi, J. E. Parks, M. J. Lance, T. J. Toops, M. D. Amiridis, *Appl. Catal. B Environ.* **2014**, *147*, 698–710.
[41] N. Lazouski, M. Chung, K. Williams, M. L. Gala, K. Manthiram, *Nat. Catal.* **2020**, *3*, 463–469.
[42] B. H. R. Suryanto, K. Matuszek, J. Choi, R. Y. Hodgetts, H. L. Du, J. M. Bakker, C. S. M. Kang, P. V. Cherepanov, A. N. Simonov, D. R. MacFarlane, *Science (80-.).* **2021**, *372*, 1187–1191.
[43] K. Aihara, M. Akiyama, T. Deguchi, M. Tanaka, R. Hagiwara, M. Iwamoto, *Chem. Commun.* **2016**, *52*, 13560–13563.
[44] N. J. Suchak, J. B. Joshi, *AIChE J.* **1994**, *40*, 944–956.
[45] E. Vervloessem, Y. Gorbanev, A. Nikiforov, N. De Geyter, A. Bogaerts, *Green Chem.* **2022**, *24*, 916–929.
[46] L. Wang, M. Xia, H. Wang, K. Huang, C. Qian, C. T. Maravelias, G. A. Ozin, *Joule* **2018**, *2*, 1055–1074.
[47] C. Philibert, *Renewable Energy for Industry: From Green Energy to Green Materials and Fuels*, Internationan Energy Agency, **2017**.
[48] N. Britun, V. Gamaleev, M. Hori, *Plasma Sources Sci. Technol.* **2021**, *30*, 08LT02.
[49] M. De Prins, E. Verheyen, A. Hoffmann, G. Vanbutsele, S. P. Sree, S. Kerkhofs, L. Van Tendeloo, F. W. Schütze, J. Martens, *J. Catal.* **2020**, *390*, 224–236.